Journal Pre-proofs

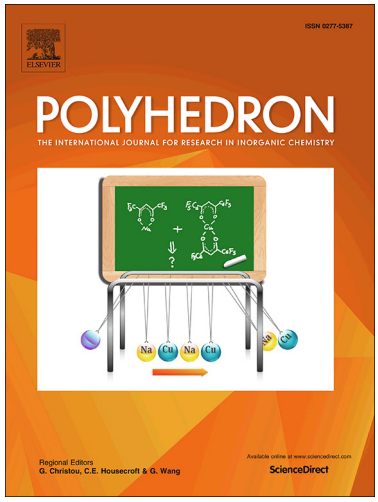

An investigation on geometry and metal interactions in multi metallic porphyrin complexes – EPR Studies [microwave power saturation and degree of covalency]

S. Tamijselvy

PII: S0277-5387(19)30740-5
DOI: https://doi.org/10.1016/j.poly.2019.114295
Reference: POLY 114295

To appear in: *Polyhedron*

Received Date: 11 September 2019
Revised Date: 27 November 2019
Accepted Date: 28 November 2019

Please cite this article as: S. Tamijselvy, An investigation on geometry and metal interactions in multi metallic porphyrin complexes – EPR Studies [microwave power saturation and degree of covalency], *Polyhedron* (2019), doi: https://doi.org/10.1016/j.poly.2019.114295

An investigation on geometry and metal interactions in multi metallic porphyrin complexes – EPR Studies [microwave power saturation and degree of covalency]

S. Tamijselvy*

School of Basic Sciences, Department of Chemistry, VISTAS, Chennai, TamilNadu-600 117, India.

Corresponding Author Tel: +91 6379647596 Email: tamijselvy@gmail.com

Abstract

Innovative stylish materials can be synthesized and designed at the molecular level by attaching well characterized and tailored functionalities that have various applications. A series of *meso*-tetracuperated porphyrin-Schiff base complexes has been prepared from metallo-5,10,15,20-tetrakis(4-hydroxyphenyl) porphyrins (M = Cu(II), VO(II) and Ni(II)) and salicylideneamino-2-(N,N-dimethylamino)ethane copper(II) perchlorate under a nitrogen atmosphere and their electron paramagnetic resonance (EPR) spectra have been studied. The steric hindrance and electronic effects of the substituted groups and the characteristics of the different metal ions are the major patrons in inducing the properties of the compounds. From detailed spectral analysis and complete simulation, the results reveal a dipolar interaction between the central copper metal ion of the porphyrin and the *meso*-copper ions, but no interaction between the vanadyl group and the *meso*-copper ions. Through studying the EPR properties of these compounds, it is clear that novel EPR oximetry materials can be found and this will help to extend the applications of EPR in vivo.

Keywords: Tetracuperated, porphyrin, Schiff base complex, EPR spectra.

Introduction

Porphyrins and their derivatives have an exceptional ability to bind a wide variety of metals and paramagnetic ligands, affording a wide range of redox photophysical and chemical properties.[1] Due to this combination of properties, porphyrin complexes are interesting in many fields of research, including the conservation of solar energy[2-6] and

electron transfer processes.[7-10] Special attention is paid to the fascinating property of the self-organization of porphyrins and metalloporphyrins, which leads to the formation of supramolecules and nano-scale porphyrin assemblies.[11] The modification of a porphyrin with ligands forms the basis of the coordination geometry, thereby changing the planarity of the complex hence formed. The non-planar conformation of metallo-porphyrins plays a vital role in determining the biotic components and the function of tetrapyrrole cofactors in proteins. The eventual interest is in the relationships between the macrocycle planarity and the reactivity of tetrapyrrole-containing biological systems, such as the special pair in the photo-synthetic reaction center heme (Fe porphyrins) in hemoproteins and cofactor F430 in methanogenic bacteria. The dominant metals are iron and copper, being most abundant in biological systems. These species are distinguishable by EPR spectroscopy through the interaction of electron spin and their different orbital arrangements.

The EPR spectrum arises from the energy difference, ΔE, between the two possible spin states, Ms = +1/2 and Ms = −1/2, of an electron when an external magnetic field is applied. Under proper conditions, a transition between these two levels can be obtained by applying an oscillating electromagnetic field with a resonant energy equal to ΔE. The value of ΔE depends on the surroundings of the hypothetical 'free' electron. It is necessary that electron must not be paired as this would dissolve the magnetic moment of either electron, both being lined up with mutually opposite spins. Two very important parameters are the spectroscopic index (g value) and the hyperfine constants (A values), both of which represent monograms for different paramagnetic species. The g-value is indicative of an electronic interaction between the unpaired electron and the applied magnetic field. For the 'free' electron, the value for g (g_e) is 2.0023, called 'free spin'. Because there are several features connected with the electron, (for example, the nucleus, orbital motion and other electrons) true g-values are different from g_e. The hyperfine coupling constants (A) measure the

connections between the electron and its nucleus and also nuclei of adjacent atoms directly bonded or further away. Further details on the theory of EPR spectroscopy can be found in the literature.[12,13]

Materials and methods

The experimental procedure and scheme for the synthesis of the desired porphyrin complexes and various characterisation techniques, such as ^{1}H-NMR spectra of the free porphyrins, FAB mass spectra, electronic absorption spectra, IR spectra, elemental analyses (C, H and N) and electrochemical experiments were discussed in an earlier report.[14] X-band EPR spectra were recorded with a JEOL JES-TES 100 ESR spectrometer having 100 kHz field modulation. Spectra at liquid nitrogen temperature were performed in a cold finger Dewar. WinEPR SimFonia software was used for the simulation of the EPR spectrum obtained at 77 K. Analysis of the intensity variation of the microwave power saturation was done for the peak at 354 mT of the vanadyl copper complex, with varying powers.

Results and discussion

In the absence of a single crystal structure, Fig. 1 shows the speculative molecular structure of the various synthesized complexes. Compounds **VI**, **VII**, **VIII** and **IX** are stable in air and are soluble in almost all non-polar organic solvents, in contrast to the parent porphyrins (**II** - CuThPP, **III** - VOThPP) and salicylideneamino-2-(N,N-dimethylamino)ethane copper(II) perchlorate (**V** - CuL), which are soluble only in polar solvents.

Electron Paramagnetic Resonance studies [EPR]

The EPR spectra were recorded for solution and polycrystalline powders of the prepared complexes at room temperature and at liquid nitrogen temperature. The EPR spectra of the polycrystalline powders of all the metalloporphyrins at room temperature show

featureless broad lines. Also, the solution spectra in ethanol/dichloromethane at room temperature show isotropic g and A values. Since these spectral patterns do not reveal any additional information, no further discussions are made. The ethanolic frozen solution EPR

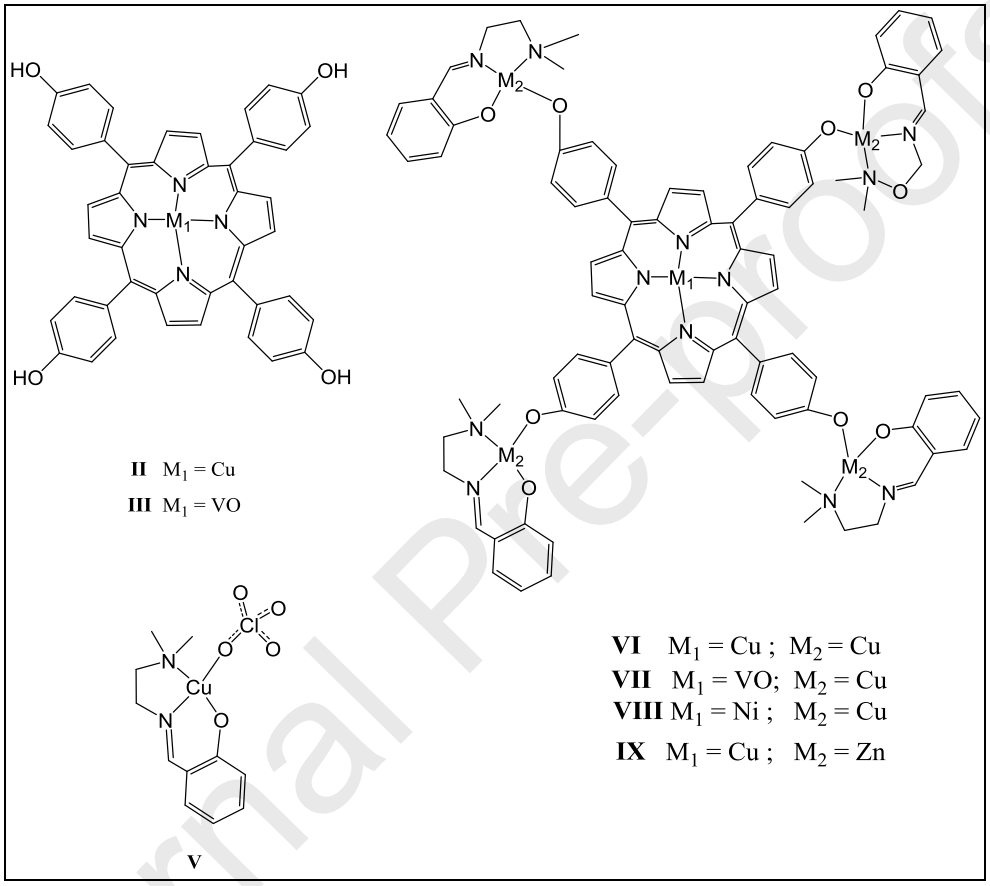

Fig1. Speculative molecular structure of the synthesized complexes

spectrum of **II** shows a typical axially symmetric Cu(II) ion spectrum for coordination at the center of the porphyrin core. The unpaired electron in the $d_{x^2-y^2}$ orbital of the copper(II) ion, with the electronic ground state $^2B_1$, gives rise to two sets of metal hyperfine lines corresponding to $g_{\|}$ and $g_{\perp}$ values. The first two components of the four copper hyperfine lines in the parallel region are well resolved in the low field region and the third component is slightly merged with the much stronger perpendicular line to a different extent, while the

fourth parallel line is completely overlapped. The appearance of super hyperfine lines from the four nitrogen atoms indicates the coordination of the copper ion at the center of the porphyrin core. A simulation of the EPR spectrum allowed us to estimate accurately the spin Hamiltonian parameters as $g_{\|}$ = 2.190, $A_{\|}^{Cu}$ = 19.63 mT, $A_{\|}^{N}$ = 1.98 mT, $g_{\perp}$ = 2.045, $A_{\perp}^{Cu}$ = 3.4 mT and $A_{\perp}^{N}$ = 1.42 mT; these values are summarized in Table 2. The observed trend is in conformity with earlier results.[15] The EPR spectrum of an ethanolic solution of **V** at 77 K also shows a similar four line pattern and the spin Hamiltonian parameters are estimated through simulation as $g_{\|}$ = 2.260, $A_{\|}^{Cu}$ = 18.5 mT, $A_{\|}^{N}$ = 1.30 mT, $g_{\perp}$ = 2.072, $A_{\perp}^{Cu}$ = 1.68 mT and $A_{\perp}^{N}$ = 1.30 mT. The observed g and A values suggest that the copper ion exists in a more distorted geometry on comparison with **II**. This geometrical distortion arises due to the flexibility of the Schiff base ligand and similar values were also observed earlier.[16]

The EPR spectrum of **VI** shows interesting results. The room temperature solution spectrum in ethanol contains four isotropic lines with g_{iso} and A_{iso} as 2.119 and 7.4mT, respectively. The frozen solution spectrum of **VI** is given in Fig. 2. The spectrum clearly reveals transitions corresponding to two types of copper ions with nearly identical spin Hamiltonian values, but with different distributions of intensity. These two types of transitions must arise from the CuThPP and CuL units of **VI**. Moreover, the spectrum has more broadening, with the complete loss of the nitrogen super hyperfine lines of CuThPP. which must arise from the interaction between the different copper centers. No additional transitions are noticed at below and above the main resonance position, indicating that the spectrum is the result of a strong dipolar interaction between the copper ions. To understand the nature of the interaction between the copper centers, three controlled experiments were performed.

Firstly, an ethanolic frozen solution spectrum of a mixture consisting of 1:4 molar ratios of **II** and **V** was obtained; spectrum could be best described as the addition of the two

spectra corresponding to **II** and **V**, showing the super hyperfine splitting from the nitrogen atoms and the resulting pattern (see supplementary figure). Secondly, the EPR spectrum of complex **VIII** was studied. This complex contains a diamagnetic metal at the central core of the porphyrin. The EPR spectrum of **VIII** nearly resembles that of pure **V** at 77 K, except that the spin Hamiltonian values are similar to that of the CuL unit in **VI**. Since, the nickel(II) ion in a square planar geometry exhibits a low spin diamagnetic state,[17] the resultant spectrum of **VIII** should reflect spin interactions between the peripheral copper ions. Since the spectrum does not show any effect, except for the geometrical change around the *meso*-substituted copper ions, we can conclude that interactions between the peripheral copper ions are negligible. However, it is clear that the geometry of the copper ions in **V** changes on coordination with the porphyrin. The spin Hamiltonian values of **VIII** are also given in Table 2. In this framework, the zinc porphyrin could have been an ideal choice rather than the nickel porphyrin. However, our efforts in synthesizing the tetracuperated zinc

Table 2. ESR spin Hamiltonian parameters of the metalloporphyrins and tetracuprated metalloporphyrins in ethanol at 77 K

S.No.	Complex	$g_{\parallel}$	$g_{\perp}$	$A_{\parallel}$ in mT	$A_{\perp}$ in mT	$A_{\parallel}^{N}$ in mT	$A_{\perp}^{N}$ in mT
1.	**II**	2.190	2.045	19.63	3.4	1.98	1.42
2.	**III**	1.965	1.982	16.92	5.64	0.29	0.28
3.	**V**	2.260	2.072	18.5	1.68	1.3	1.3
4.	**VI**	2.247	2.081	19.53	2.8	1.18	1.08
		2.222	2.056	19.31	3.02	1.16	1.08
5.	**VII**	1.959	1.982	17.02	5.78	0.29	0.28
		2.210	2.055	18.7	1.88	1.3	1.3
6.	**VIII**	2.230	2.054	18.0	1.7	1.025	1.025
7.	**IX**	2.170	2.040	19.6	3.3	1.97	1.42

porphyrin failed and invariably compound **VI** resulted. This must be due to *trans* metallation of zinc by copper at the porphyrin center.[18] Thirdly, a complex with a paramagnetic metal at the porphyrin core and a diamagnetic metal at the periphery has been synthesized (**IX**). Substitution of a diamagnetic metal ion (the Zn^{2+} ion) at the peripheral position did not alter the spectrum of the copper ion at the porphyrin core and spectrum matches well with the spectrum of **II**. The above three control experiments suggest the following properties. (i) Peripheral metal substitution alone does not bring about loss of the nitrogen hyperfine splitting of the central copper ion (as shown in **IX**), (ii) the interactions between peripheral copper centers are very negligible with no drastic modification in the EPR spectrum (as shown in the case of **VIII**). This observation is quite common for paramagnetic metal centers in diamagnetic hosts[19,20] and in macro-cycle ligand systems.[21] To further confirm the non-interacting behaviour among the peripheral copper ions, a microwave power saturation recovery study has been carried out. This technique involves a study of the intensity of the EPR transition lines as a function of microwave power. The area of the resonance line was plotted against the microwave power. The experimental data were fitted to the following equation, employing non-linear least square fitting:

$$I = \left(\frac{a\sqrt{p}}{1 + \frac{p}{b}} \right)^{\frac{c}{2}} \qquad (1)$$

where '*a*' is the coupling constant, '*b*' is the value of the microwave power '*p*' such that the intensity *I*, measured experimentally, falls to half the value that should be attained in the absence of saturation and *'c*' indicates the degree of homogeneity of the spin systems. The parameter '*c*' assumes values between 1, completely homogeneous, and 2, completely inhomogeneous, at low microwave power. We could relate[22] the value of *b* to the measure of

the spin relaxation times by the relation $b = \gamma^2 B^2 T_1 T_2$, where γ is gyro magnetic ratio, B is the applied magnetic field, T_1 is the spin lattice relaxation time and T_2 is the time constant of the

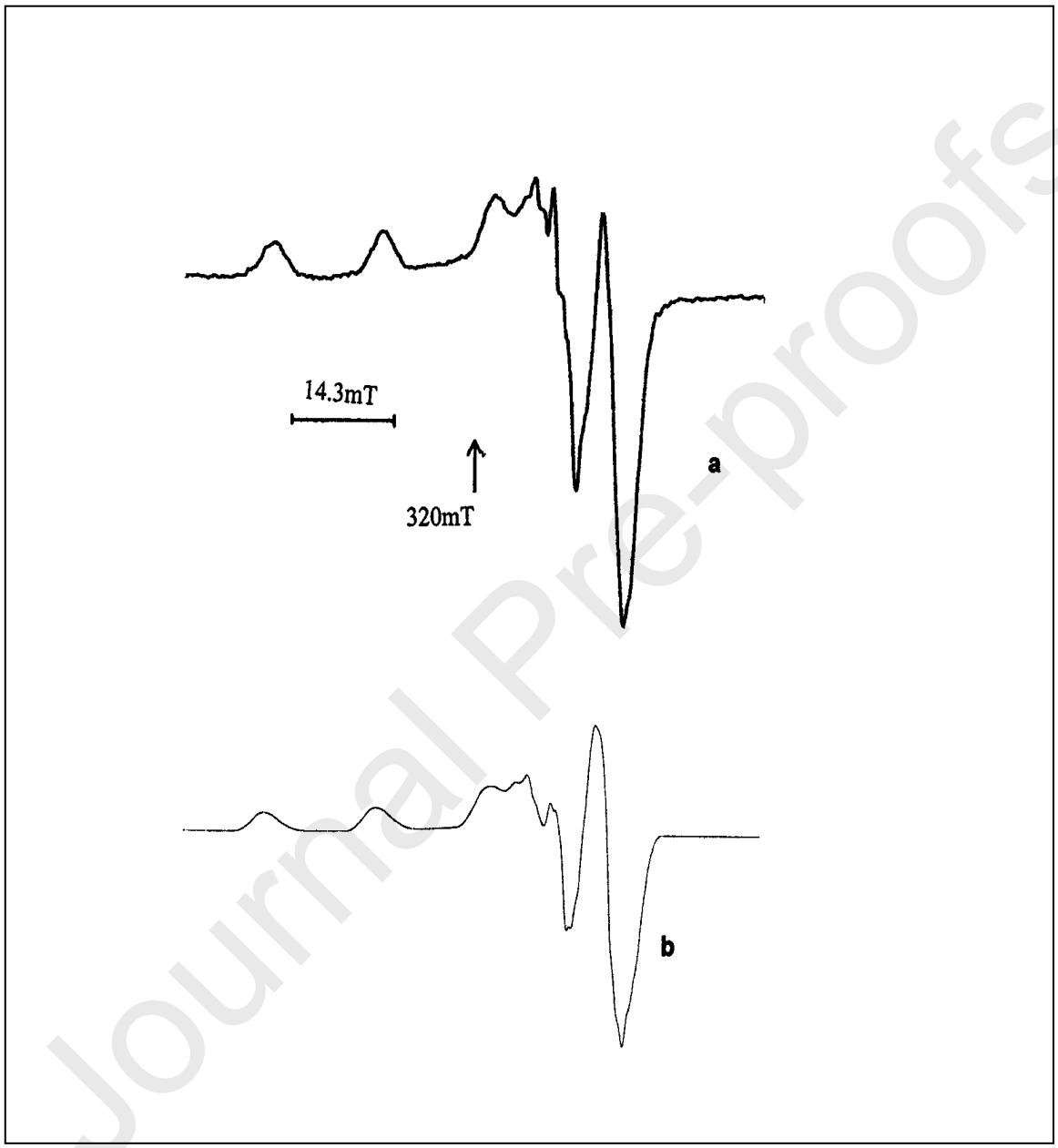

Fig. 2. EPR spectrum of **VI** in ethanol at 77 K. (a) experimental; (b) simulated. The simulation parameters are $g_{\parallel}$ = 2.247, 2.222, $g_{\perp}$ = 2.081, 2.056, $A_{\parallel}^{Cu}$ = 19.5, 19.3 mT, $A_{\perp}^{Cu}$ = 2.8, 3.0 mT, $A_{\parallel}^{N}$ = 1.18, 1.16 mT, $A_{\perp}^{N}$ = 1.08, 1.08 mT, line width: parallel =1.25, 1.6mT, perpendicular = 1.35, 1.6 mT. ν = 9.056 GHz

rate of attainment of the equilibrium when the spin relaxes within the spin system. The *b* values estimated for **II** and **V** were found to be 6.08 and 1.88 mW, respectively. The *b* value for **VIII** was found to be 1.54 mW, which is quite similar to that of **V**. The small deviation in the value in **VIII** may be due to some structural changes to attain planarity. The *b* value for **IX** was found to be 6.12 mW, which is similar to that of **II**, indicating the same electronic nature of the copper ion in both **II** and **IX**.

Assuming that the interactions between the peripheral copper ions in **VI** are negligible, we simulated the spectrum considering two types of copper ions with line broadening due to a dipole interaction between the central copper ion and the peripheral copper ions. The simulated spectrum is given in Fig. 2b. One can see a good agreement between the experimental and simulated spectra. Firstly, the $g_{\|}$ values are found to be 2.247 and 2.222 for the CuThPP and CuL units respectively. Similar changes in $g_{\perp}$ values are also noted and the values are 2.081 and 2.056 for CuThPP and CuL respectively. In comparison with the values of the respective parent compounds, the CuThPP unit shows an increase in the $g_{\|}$ and $g_{\perp}$ values, while the CuL unit shows a decrease. Since, the g values of both moieties approach each other, it is clear that both sets of copper ions stabilize in a similar geometry. Secondly, in comparison with the parent compound **V**, the $A_{\|}$ value of the CuL unit in **VI** increases from 18.5 to 19.3 mT, which strongly suggests that the copper ion in CuL adapts a more planar geometry than in **V**. Also, the $A_{\perp}$ value increases from 1.68 to 3.02 mT, and this large increase indicates a more axially symmetric nature of the peripheral copper ions in **VI** than in **V**. This means that the copper ion of CuL in **VI** adapts a more planar geometry.[23] However, along the expected lines, the A values of the CuThPP group do not show any marked change as the copper ion already exists in a stable planar configuration.[22] Thirdly, the true line width of CuThPP in **VI**, in comparison with the parent **II**, estimated

through simulation, was found to increase from 0.5 and 0.4 mT to 1.25 and 1.35 mT for the parallel and perpendicular lines respectively. This increase in the line widths is responsible for the loss of the nitrogen super hyperfine lines in **VI**. However, the line width of CuL in **VI** is found to be nearly same, at 1.6 mT, as observed in **V**. Since, it is clear that the peripheral copper sites do not interact between themselves, as shown in the case of **VIII**, and peripheral modification alone does not bring about spectral broadening of the central copper ion, as shown in the case of **IX**, the increased broadness in the spectrum of **VI** is a clear indication of a strong dipolar interaction between the central copper and peripheral copper ions. This interaction would have been justified if a microwave power saturation study had been done to evaluate the relaxation times of the copper ions in **VI**. However, the overlap of both the central and peripheral copper ions peaks in **VI** forbade us to evaluate any reliable relaxation time data. However, the interaction between the central and peripheral copper ions is estimated by calculating the degree of covalency. Thus, we estimated the change in the electron density character in terms of the degree of covalency, α^2, in various bonds through the well-known equation (2),[24] in which the $A_{\parallel}$ values are taken in units of cm^{-1}.

$$\alpha^2 = (A_{\parallel} / 0.036) + (g_{\parallel} - 2.0023) + 3/7\ (g_{\perp} - 2.0023) + 0.04 \qquad (2)$$

The α values are found to be 0.88 for **II** and 0.92 for **VI**, indicating that the Cu-N bonds at the porphyrin core are slightly more covalent in **VI** than in **II**. This increased covalency must be occurring by adopting a more planar geometry, thus resulting in more delocalization of the metal non-bonding electron density towards the porphyrin π structure. The corresponding α values for the CuL unit in **V** and **VI** are 0.92 and 0.91, respectively, indicating no major change. Thus it is clearly indicated that there is an interaction which results in a shift in the electron density from copper ion towards the porphyrin π system. In this context, it is

worthwhile to take a note of a similar dipolar interaction observed in a bi-copper complex of a bi-cyclam ligand.[25]

The EPR behaviour of **VII** is found to be different from that of **VI**, as shown in Fig 3. In the spectrum, one can see copper hyperfine lines in addition to vanadyl hyperfine lines, with an approximate 4:1 intensity ratio in the low field region. In the high field region, the spectrum is complex due to overlapped resonances. Knowing that the peripheral copper centers do not interact with each other, simulation of the EPR spectrum of **VII** was performed considering no interactions between the vanadyl and copper ions. The simulated spectrum is given in Fig. 3b and it matches exceedingly well with the experimental spectrum. The evaluated spin Hamiltonian values are $g_{\|} = 1.959$, $A_{\|}^{V} = 17.0$ mT, $A_{\|}^{N} = 0.3$ mT, $g_{\perp} = 1.982$, $A_{\perp}^{V} = 5.64$ mT and $A_{\perp}^{N} = 0.3$ mT. The corresponding values for the CuL units are $g_{\|} = 2.210$, $A_{\|}^{Cu} = 18.7$ mT, $A_{\|}^{N} = 1.30$ mT, $g_{\perp} = 2.055$, $A_{\perp}^{Cu} = 1.88$ mT and $A_{\perp}^{N} = 1.30$ mT. The values corresponding to the vanadyl porphyrin in **VII** are nearly same as those of **III**. However, the CuL values are similar to those observed in **VI**. Thus, it is clear that the interaction between the vanadyl and *meso*-copper ions is much weaker than between the copper ions in **VI**. The high magnetic field parallel lines of the vanadyl ion, which are free from any copper hyperfine lines, helped us to evaluate a qualitative measure of the relaxation time of vanadium through a microwave power saturation recovery technique.[26] The values of *b* (calculated using equation 1) were found to be 460 and 510 mW for **VII** and **III**, respectively and *c* was found to be 0.99, indicating a near homogeneous spin system. The nearly same value of *b* in both **VII** and **III** indicates that the spin-spin interaction is nearly zero; otherwise one would have seen a large reduction in the *b* value for **VII**.

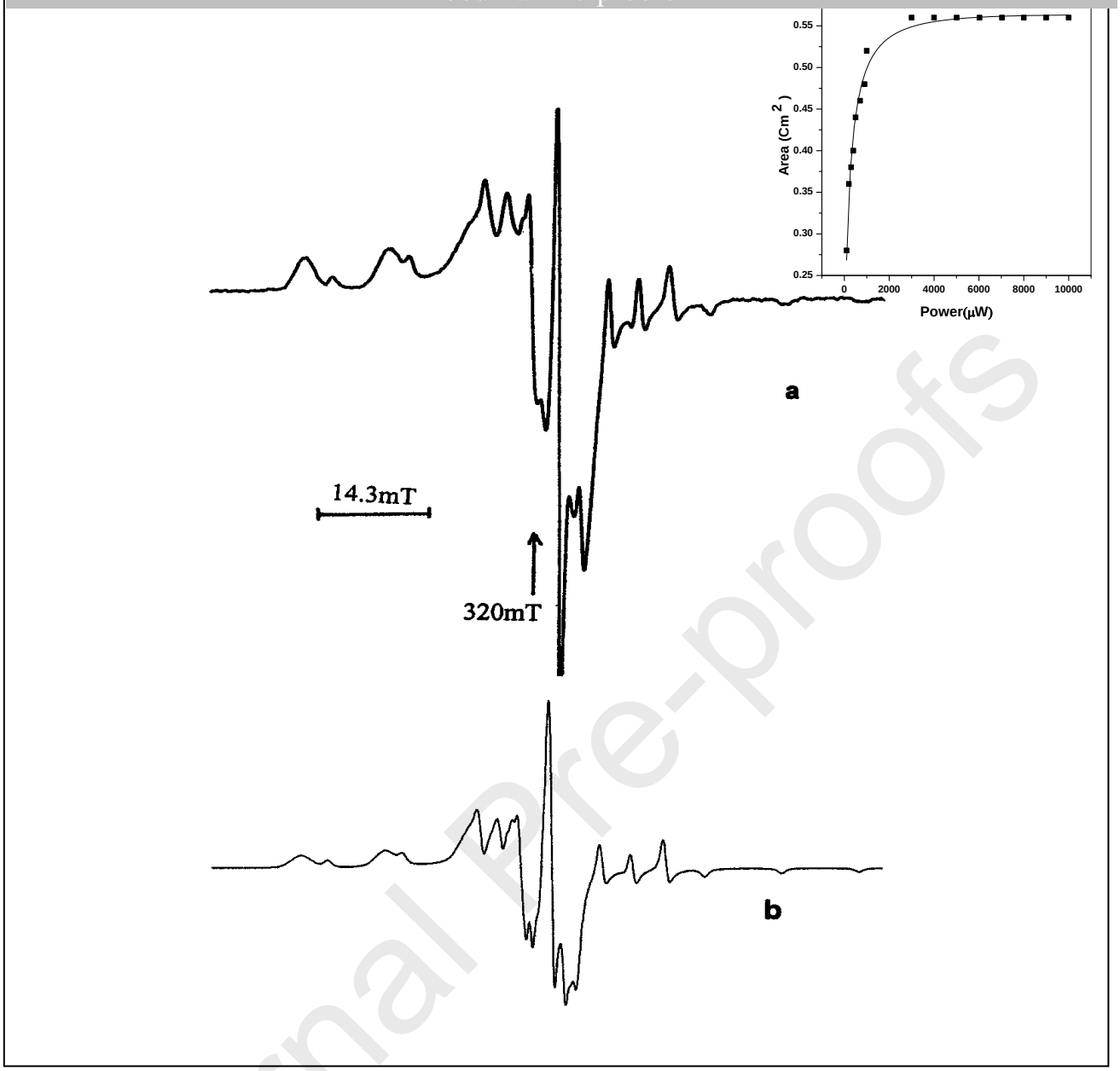

Fig. 3. ESR spectra of **VII** in ethanol at 77 K. (a) experimental; (b) simulated. The simulation parameters are $g_{\parallel}$ = 1.959, 2.210, $g_{\perp}$ = 1.982, 2.055, $A_{\parallel}^{V}$ = 17.0 mT, $A_{\parallel}^{Cu}$ = 18.7 mT, $A_{\perp}^{V}$ = 5.78 mT, $A_{\perp}^{Cu}$ = 1.88 mT, $A_{\parallel}^{N}$ = 0.3, 1.3 mT. $A_{\perp}^{N}$ = 0.3, 1.3 mT. Line width: parallel = 0.8, 1.4 mT, perpendicular = 0.65, 1.4 mT. ν = 9.059 GHz; (c) microwave power saturation recovery plot at 77 K of 0.5 mM for the peak of **VII** at 354 mT. Solid line represents the theoretical fit to the equation $I = [a\,(P)^{1/2}/(1+P/b)]^{c/2}$

It is interesting to explain why the extent of the interactions are different in **VI** and **VII**. In the case of the all copper system, the unpaired electron occupies the $d_{x^2-y^2}$ orbital because of the square planar geometry around copper ions. In contrary, the unpaired electron of the square pyramidal vanadyl(II) ion in the porphyrin occupies the out of plane d_{xz} or d_{yz} orbital, thus minimizing the interaction with the copper(II) ion.

Conclusion

Electronic ground state interactions between the all copper and vanadyl-copper poprhyrin are negligible, which is clearly understood from EPR studies. The peripheral copper ion interacts more strongly with the central copper ion than with the central vanadyl ion. This was confirmed from the power saturation study. The occupation of the unpaired electron of the central metal ion varies between copper and vanadium, making the complex change in geometry and also giving a variation in the interaction between the central and peripheral metal systems. These interactions of the metal center and thereby the change in the planarity could make this compound work as a better catalyst. Also, it could be used to monitor pO_2 continuously and/or repeatedly at exactly the same localized area in tissue *in vivo* without the need for anesthesia, as a change in planarity occurs for even a small difference in pO_2, i.e. at the very low levels that occur pathophysiological, and that can be used in a variety of settings. However, proof for all these applications has yet to be performed.

Acknowledgment

Author thanks UGC for a fellowship, Dr. R. Venkatesan and Dr. J. Subramanian for helpful discussions during the EPR simulations.

References

1. K.M. Kadish, K.M. Smith, R. Guilard (eds.), The Porphyrin Handbook, vol 1–20 (Acad. Press, NewYork, 2000–2003)
2. D. Gust, Nature 1997, **386**, 21.
3. J.A.A.W. Elemans, R. van Hameren, R.J.M. Notle, A.E. Rowan, Adv. Mater. 2006, **18**, 1251.
4. N. Krauss, W. Hinrichs, I. Witt, P. Fromme, W. Pritzkow, Z. Dauter, C. Betzel, K.S. Wilson, H.T. Witt, W. Saenger, Nature 1993, **361**, 326.
5. G. McDermott, S.M. Prince, A.A. Freer, A.M. Hawthornthwaite-Lawless, M.Z. Papiz, R.J. Cogdell, N.W. Isaacs, Nature 1995, **374**, 517.
6. P. Jordan, P. Fromme, H.-T. Witt, O. Klukas, W. Saenger, N. Kraub, Nature 2001, **411**, 909.
7. A.P.S. Samuel, D.T. Co, C.L. Stern, M.R. Wasielewski, J. Am. Chem. Soc. 2010, **132**, 8813.
8. T. Honda, T. Nakanishi, K. Ohkubo, T. Kojima, S. Fukuzumi, J. Phys. Chem. C 2010, **114(33)**, 14290.
9. K. Mobius, W. Lubitz, A. Savitsky, Appl. Magn. Reson. 2011, **41(2–4)**, 113.
10. P.K. Poddutoori, N. Zarrabi, A.G. Moiseev, R. Gumbau-Brisa, S. Vassiliev S, A. Van der Est, Chemistry 2013, **19(9)**, 3148. doi:10.1002/chem.201202995
11. G.M. Mamardashvili, NZh Mamardashvili, O.I. Koifman, Usp. Khimii 2008, **77(1)**, 60.
12. M. Symons, Chemical and Biochemical Aspects of Electron-Spin Resonance Spectroscopy, Van Nostrand Reinhold, England, 1978.
13. J.R. Pilbrow, Transition Ion Electron Paramagnetic Resonance, Clarendon Press, Oxford, 1990.
14. S. Tamijselvy, Research J. Pharm. Tech. 2018, **11(6)**, 2581.
15. J.Subramanian in *Porphyrins and Metallo porphyrins*, Kevin M.Smith Ed., Elsevier, Amsterdam, 1975, chapter 13
16. Sir Geoffrey Wilkinson, Robert D. Gillard and Jon A. McCleverty, *Comprehensive Coordination Chemistry*, Vol.5, p.667, A.Wheaton and Co. Ltd., Great Britain, 1987.

17. A.B.P. Lever, *Inorganic Electronic Spectroscopy*, 2nd Ed., Elsevier, Amsterdam, 1984, ch. 6, p.534.
18. J.W. Buchler in *Porphyrins and Metallo porphyrins*, Kevin M. Smith Ed., Elsevier, Amsterdam, 1975, chapter 5.
19. R. Srinivasan, E. Poonguzali, R. Venkatesan, T. M. Rajendiran, R. V.S.S. N. Ravikumar, P. Sambasiva Rao, J. Phys. Chem. Solids 2003, **64**, 1139 and references therein.
20. E. Poonguzali, R. Srinivasan, R. V. S. S. N. Ravikumar, A. V. Chandrasekar, B. J. Reddy, Y. P. Reddy, P. Sambasiva Rao, Phys. Scripta 2002, **66**, 391 and references therein.
21. Jean-Louis Pierre, Pierre Chautemps, Sidi Refaif, Claude Beguin, Abdelilah EI Marzouki, Guy Serratrice, Eric Saint-Aman, Paul Rey, J. Am. Chem. Soc. 1995, **117**, 1965.
22. J.L. Hoard in *Porphyrins and Metallo porphyrins*, Kevin M.Smith Ed., Elsevier, Amsterdam, 1975, ch. 8.
23. J.R. Pilbrow, *Transition Ion Electron Paramagnetic Resonance*, Oxford Science, New York, 1990.
24. R.L. Dutta and A. Syamal, *Elements of Magneto Chemistry*, S.Chand, New Delhi, 1990, ch. 12.
25. McAuley and S. Subramanian, M. J. Zaworotko, K. Biradha, Inorg. Chem. 1999, **38**, 5078.
26. C. Mailer, T. Sarna, H.M. Swartz, J.S. Hyde, J. Magn. Reson. 1977, **25**, 205.

Supplementary

The solution EPR spectra of the complexes at room temperature, the frozen solution EPR spectra of **II**, **III**, **V**, **VIII**, **IX** and the power saturation EPR spectrum are given as supplementary data.

Supplementary materials

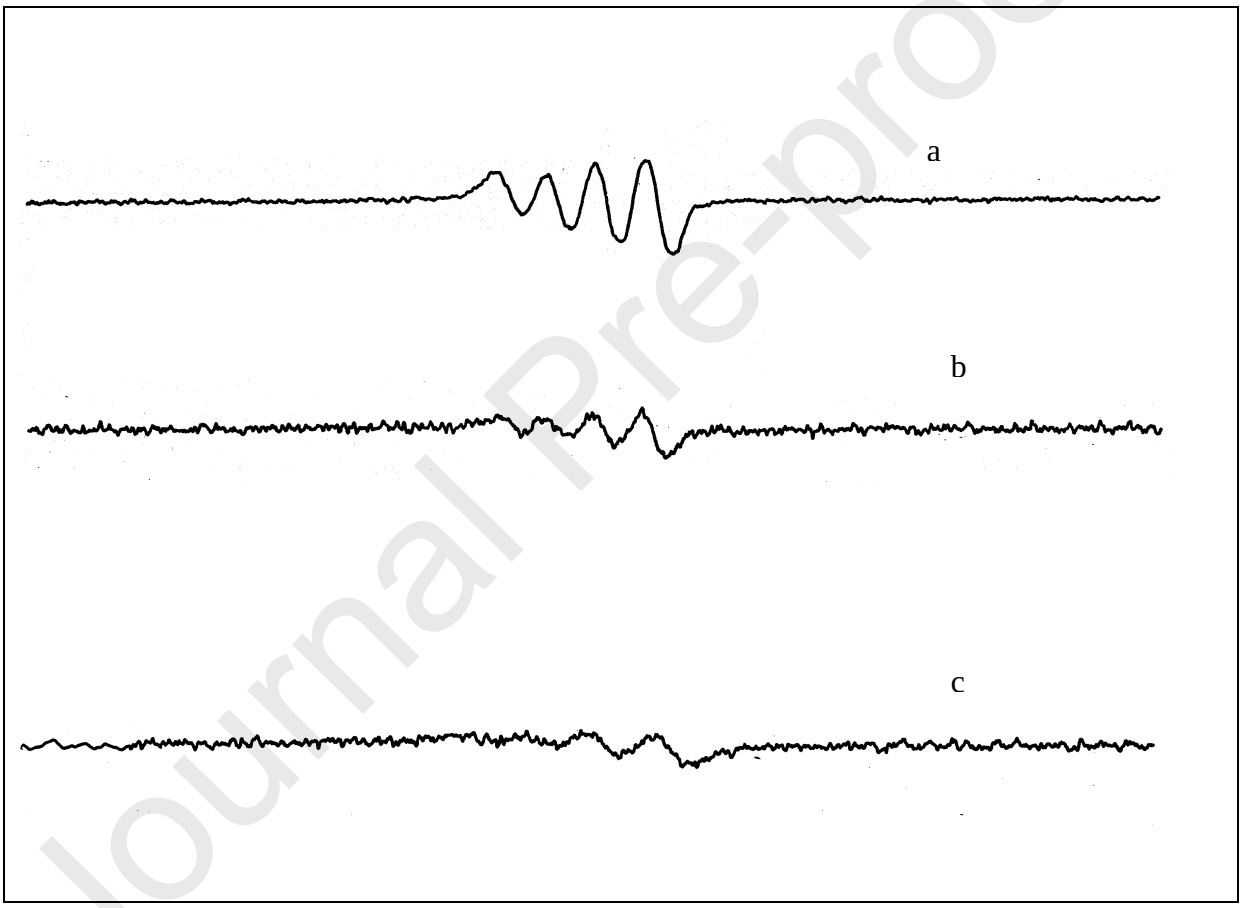

Fig S1. Room temperature EPR spectra of (a) **VI** (b) **VII** (c) **VIII** in dichloromethane.

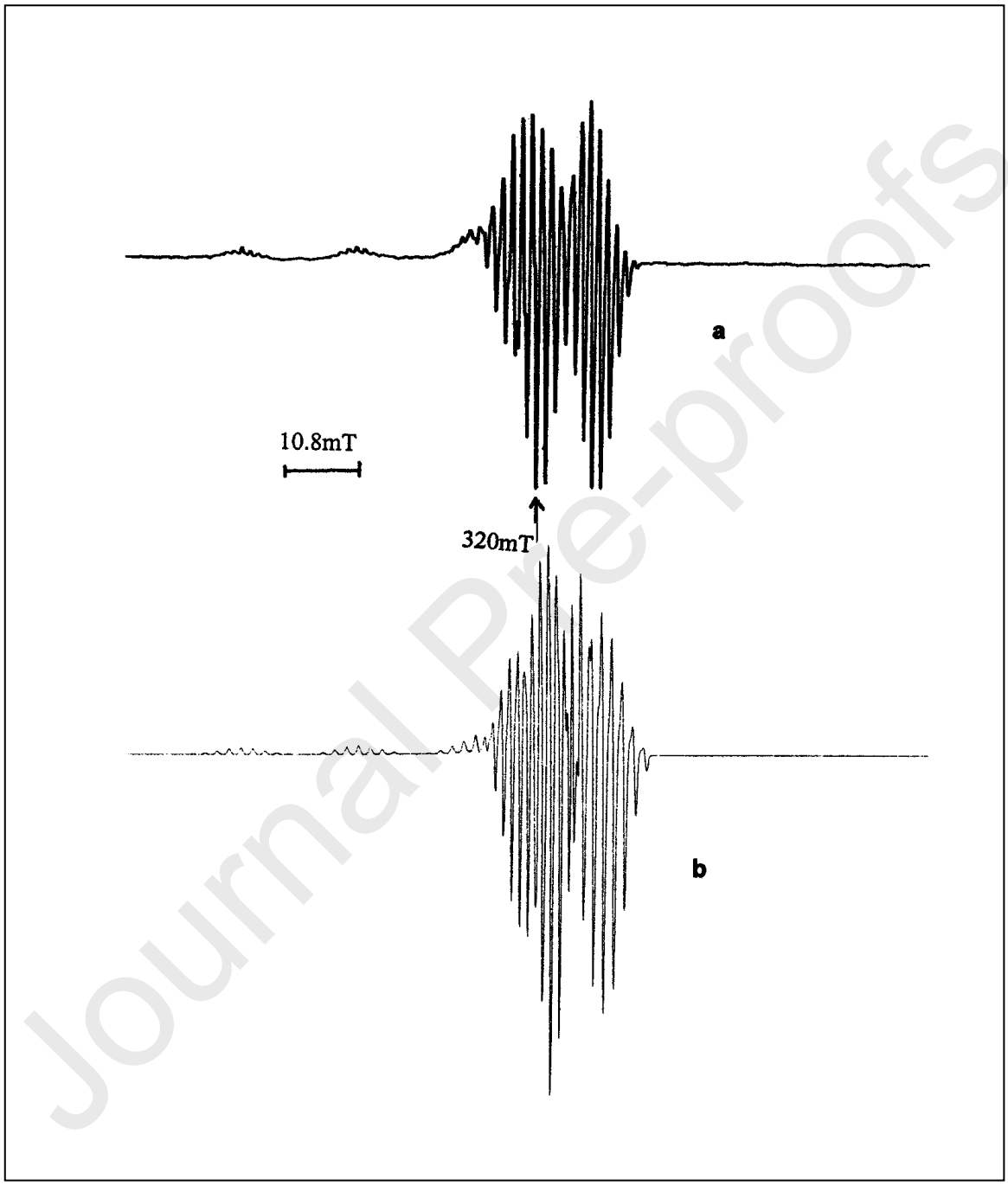

Fig S2. EPR spectra of **II** in ethanol at 77 K. (a) experimental; (b) simulated. The simulation parameters are $g_{\parallel} = 2.19$, $g_{\perp} = 2.045$, $A_{\parallel}^{Cu} = 19.6$mT, $A_{\perp}^{Cu} = 3.4$ mT, $A_{\parallel}^{N} = 1.98$ mT, $A_{\perp}^{N} = 1.42$ mT. Line width: parallel = 0.55 mT, perpendicular = 0.4 mT. $\nu = 9.062$ GHz

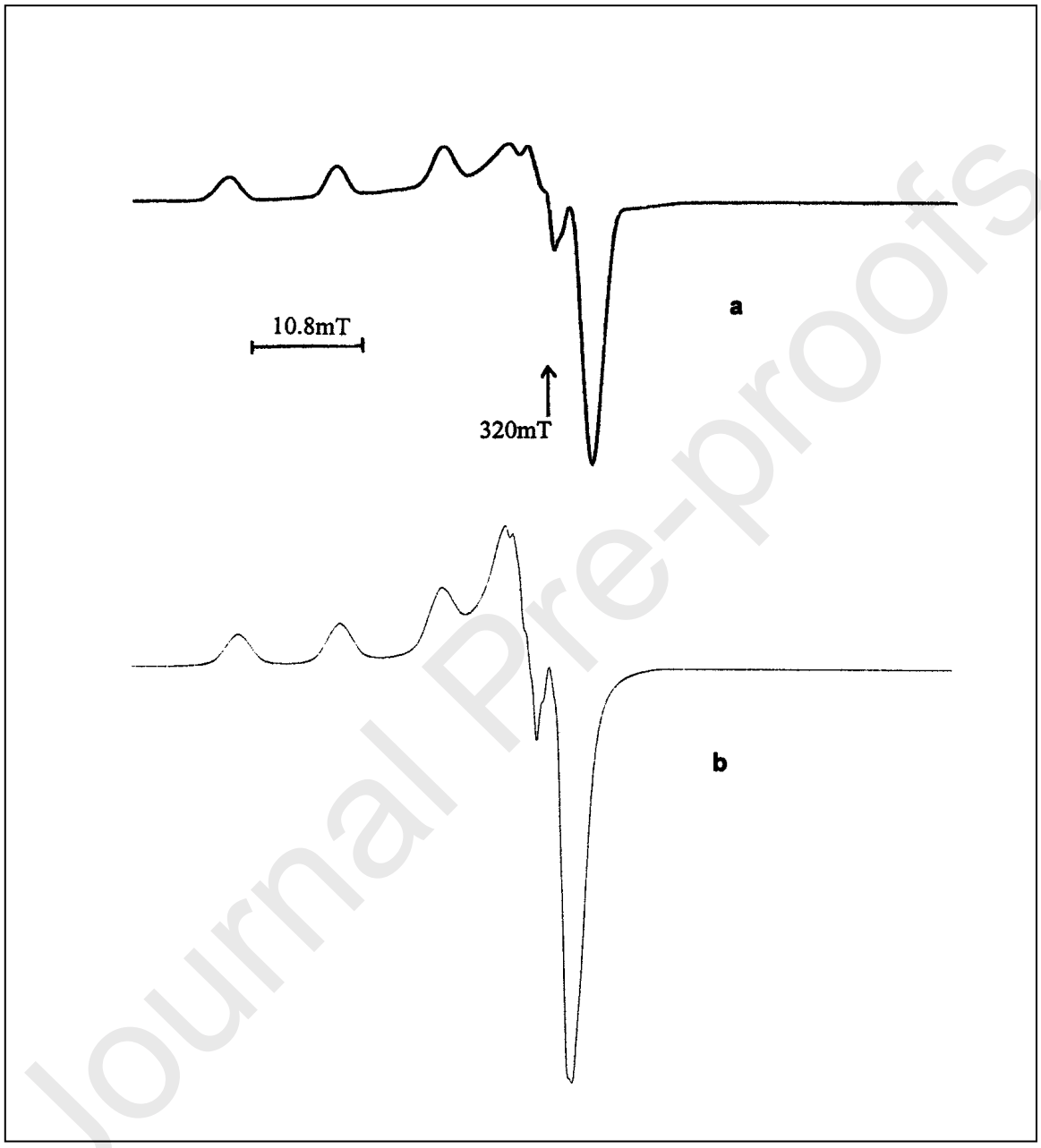

Fig S3. EPR spectra of **V** in ethanol at 77 K. (a) experimental; (b) simulated. The simulated parameters are $g_{\parallel} = 2.260$, $g_{\perp} = 2.072$, $A_{\parallel}^{Cu} = 18.5$mT, $A_{\perp}^{Cu} = 1.68$ mT, $A_{\parallel}^{N} = 1.3$ mT, $A_{\perp}^{N} = 1.3$ mT. Line width: parallel = 1.6mT, perpendicular = 1.6 mT. $\nu = 9.053$ GHz

Fig S4. EPR spectrum obtained by mixing **II** and **V** in a ratio of 1:4 in ethanol at 77 K. ν = 9.019 GHz with a centre field of 320 mT. * These hyperfine lines arise from the central copper porphyrin.

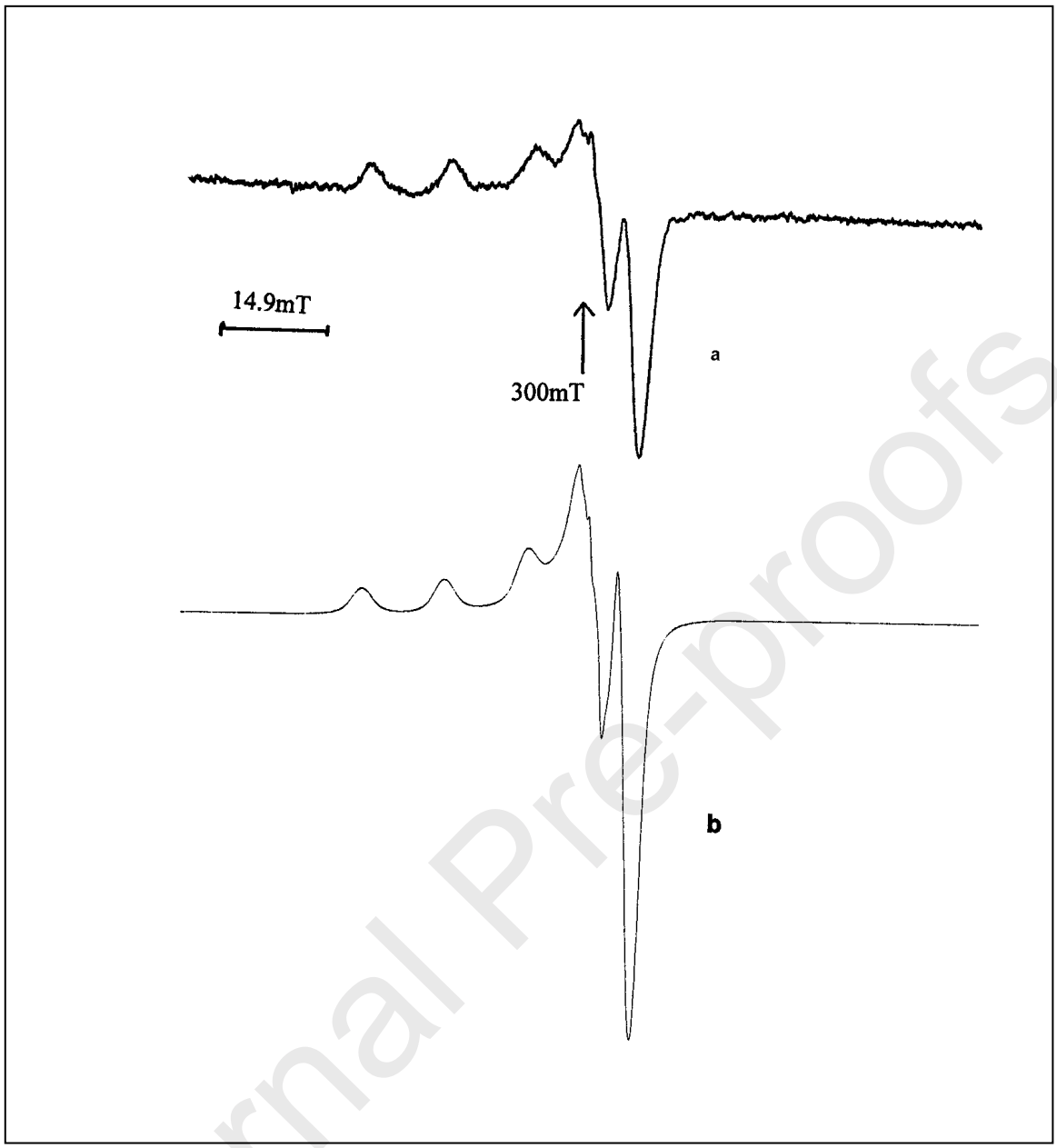

Fig S5. EPR spectra of **VIII** in ethanol at 77 K. (a) experimental; (b) simulated. The simulation parameters are $g_{\parallel} = 2.23$, $g_{\perp} = 2.054$, $A_{\parallel}^{Cu} = 18.0$ mT, $A_{\perp}^{Cu} = 1.7$ mT, $A_{\parallel}^{N} = 1.03$ mT, $A_{\perp}^{N} = 1.03$ mT. Line width: parallel = 1.6 mT, perpendicular = 1.6 mT. $\nu = 9.052$ GHz

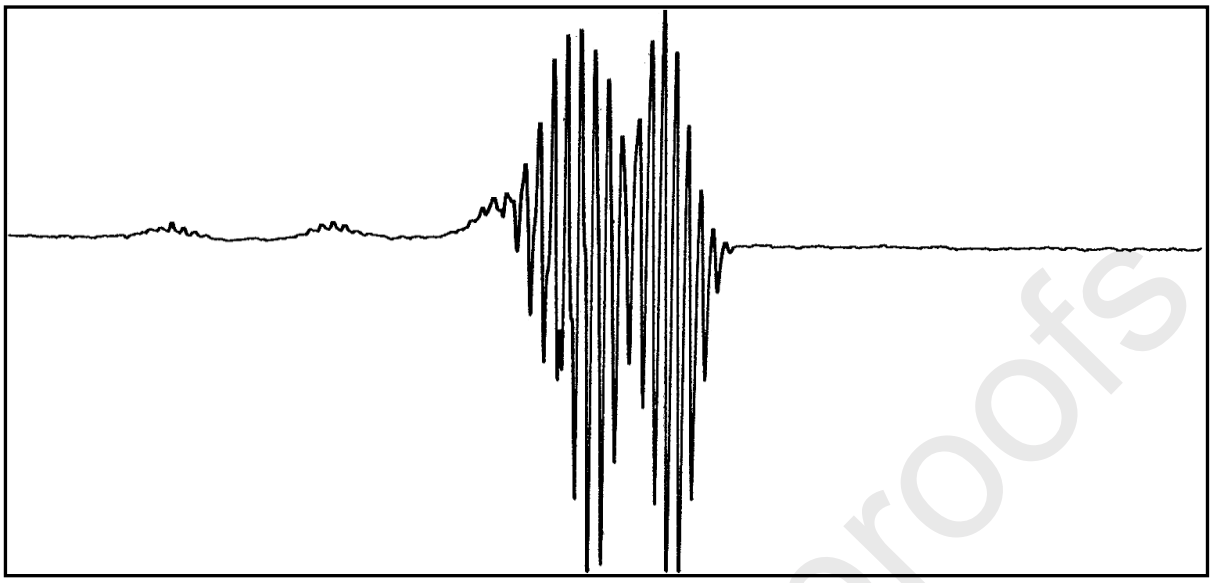

Fig S6. EPR spectrum of **IX** in ethanol at 77 K. The Hamiltonian observed $g_{\parallel} = 2.18$, $g_{\perp} = 2.040$, $A_{\parallel}^{Cu} = 19.6$ mT, $A_{\perp}^{Cu} = 3.3$ mT, $A_{\parallel}^{N} = 1.97$ mT, $A_{\perp}^{N} = 1.42$ mT. Line width: parallel = 0.5 mT, perpendicular = 0.45 mT, $\nu = 9.062$ GHz

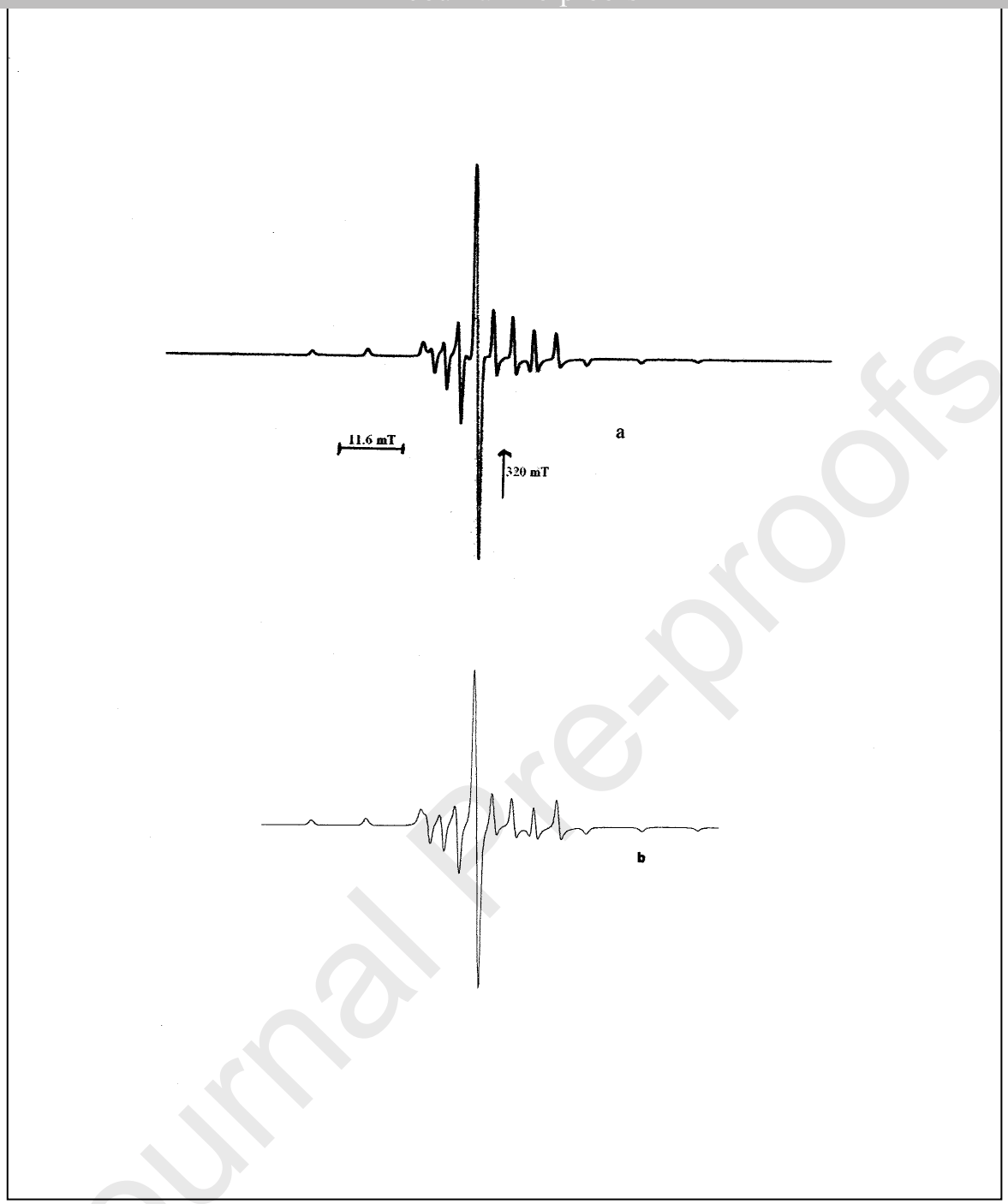

Fig S7. EPR spectra of **III** in ethanol solution at 77 K. (a) experimental; (b) simulated. The simulation parameters are $g_{\parallel} = 1.965$, $g_{\perp} = 1.982$, $A_{\parallel}^{V} = 16.9$ mT, $A_{\perp}^{V} = 5.64$ mT, $A_{\parallel}^{N} = 0.3$ mT, $A_{\perp}^{N} = 0.3$ mT. Line width: parallel = 0.6 mT, perpendicular = 0.45 mT, $\nu = 9.052$ GHz

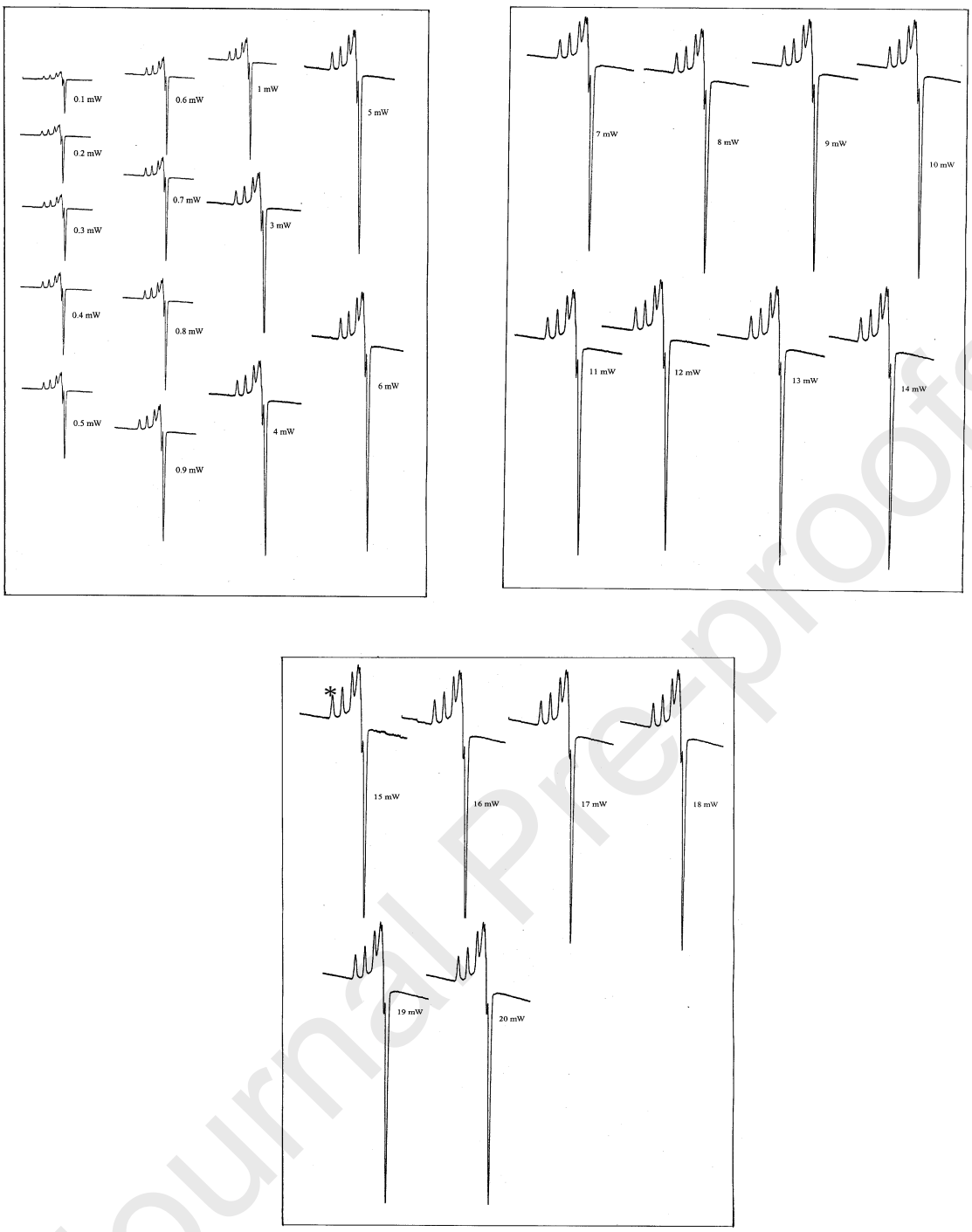

Fig S8a. Representative picture of the EPR Power Saturation spectra of **V** (0.5 mM) in an ethanolic solution at 77 K at the X-band frequency of 9.05252 GHz in the range 200 to 400 mT. * represents the peak at 261 mT used for the saturation plot.

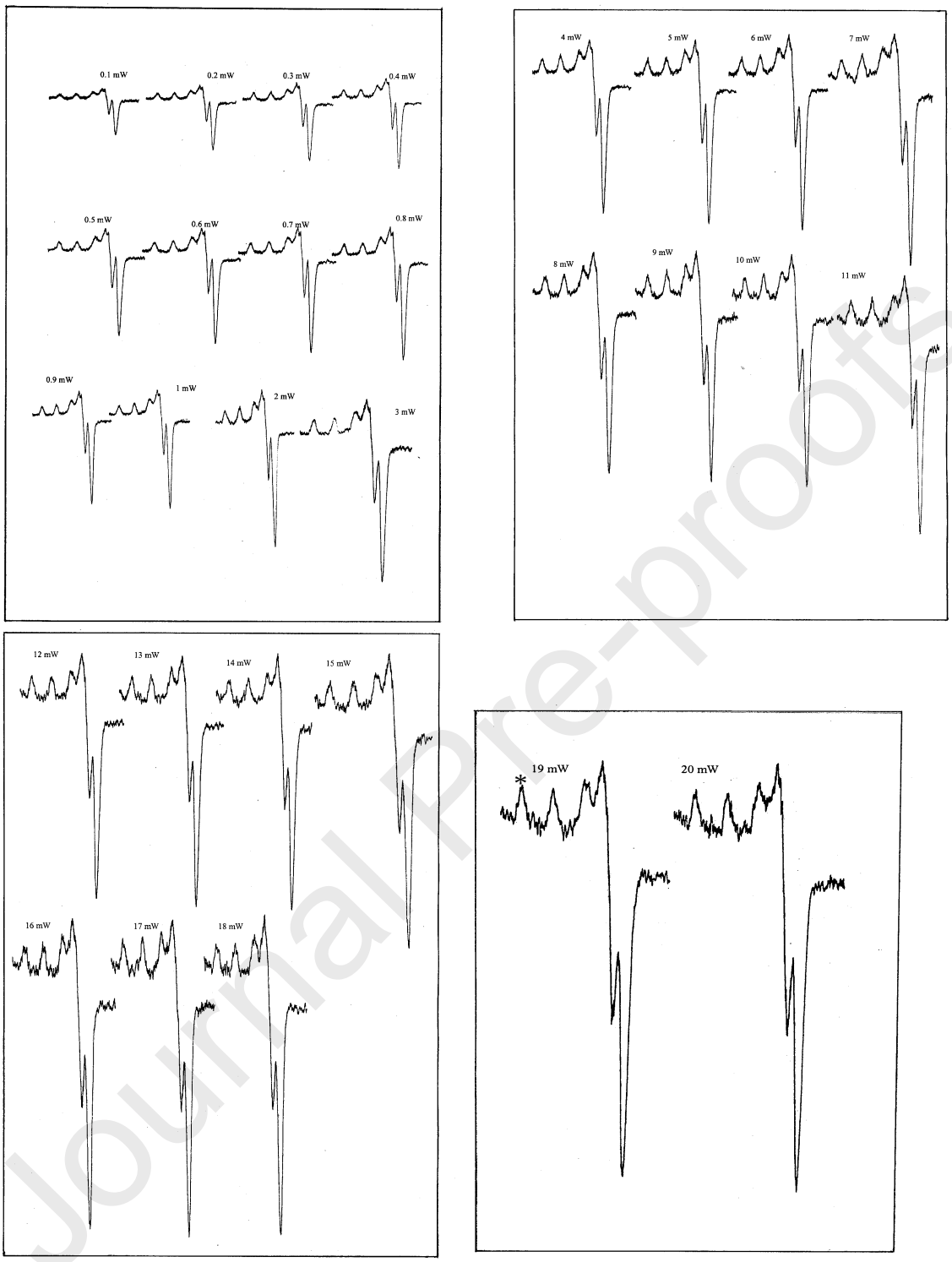

Fig S8b. Representative picture of the EPR Power Saturation spectra of **VIII** (0.5 mM) in an ethanolic solution at 77 K at the X-band frequency of 9.0518 GHz in the range 250 to 350 mT. * represents the peak at 261 mT used for the saturation plot.

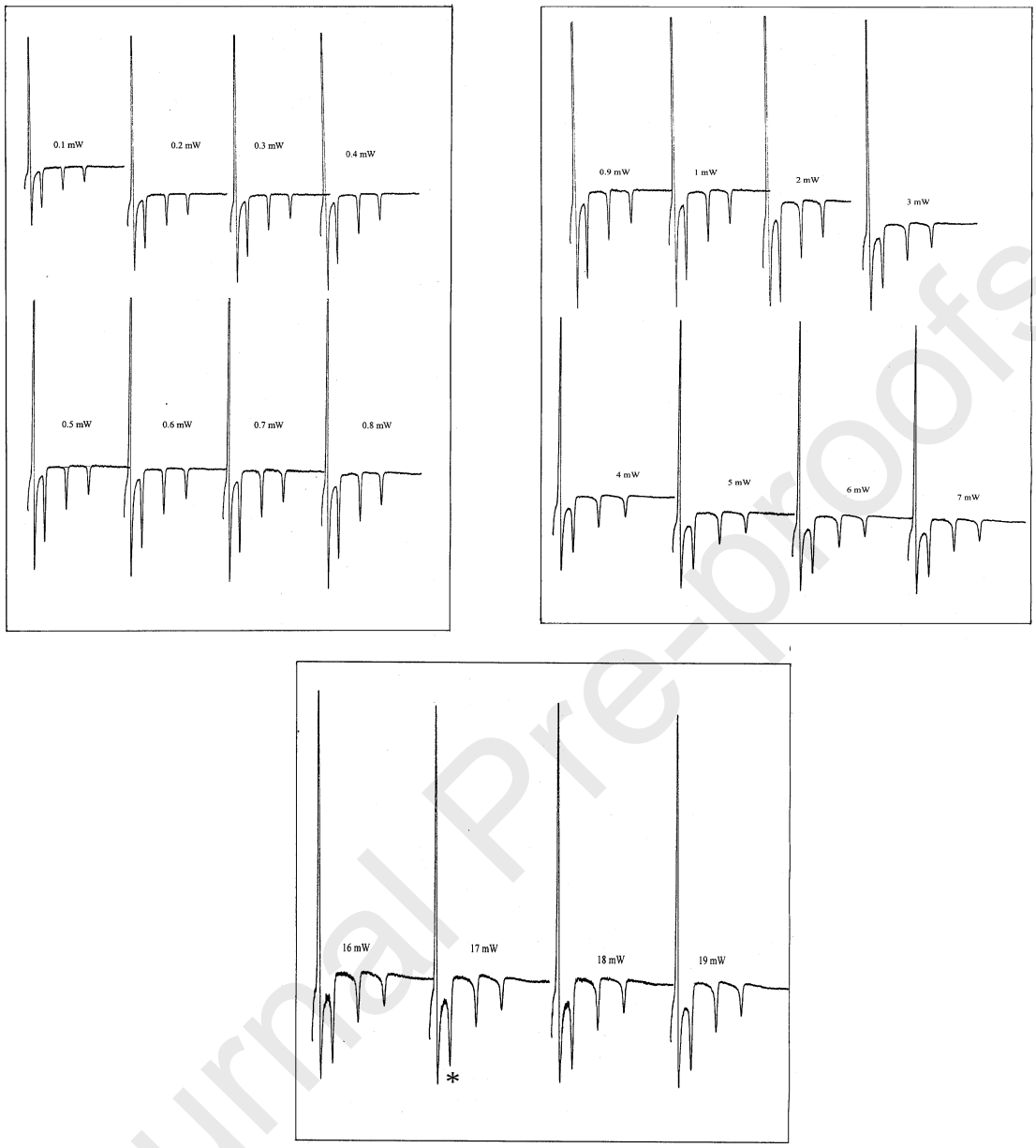

Fig S8c. Representative picture of the EPR Power Saturation spectra of **III** (0.5 mM) in an ethanolic solution at 77 K at the X-band frequency of 9.05215 GHz in the range 340 to 420 mT. * represents the peak at 354 mT used for the saturation plot.

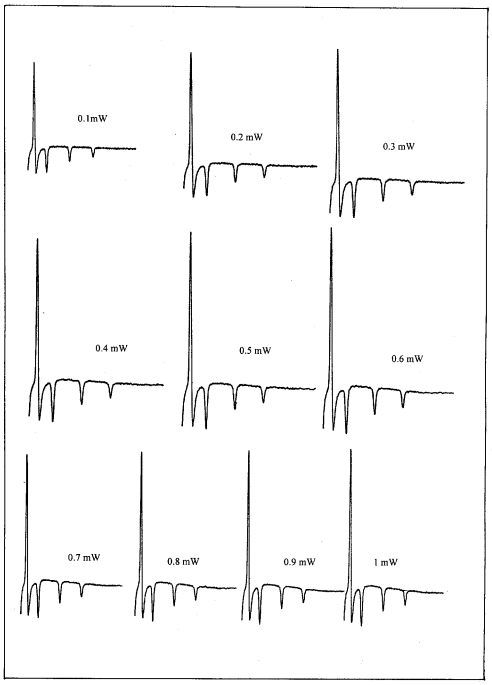

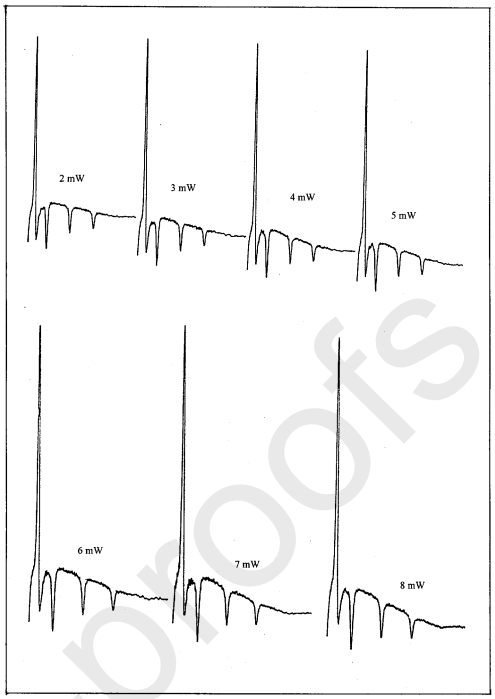

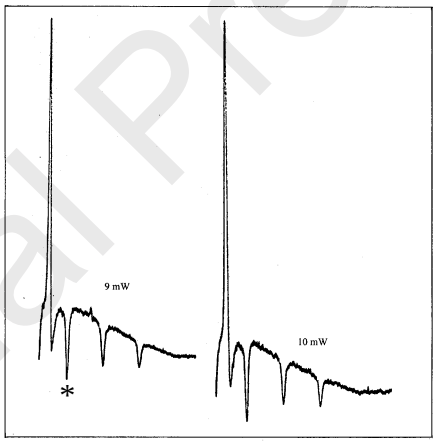

Fig S8d. Representative picture of the EPR Power Saturation spectra of **VII** (0.5 mM) in an ethanolic solution at 77 K at the X-band frequency of 9.0589 GHz in the range 340 to 420 mT. * represents the peak at 354 mT used for the saturation plot.

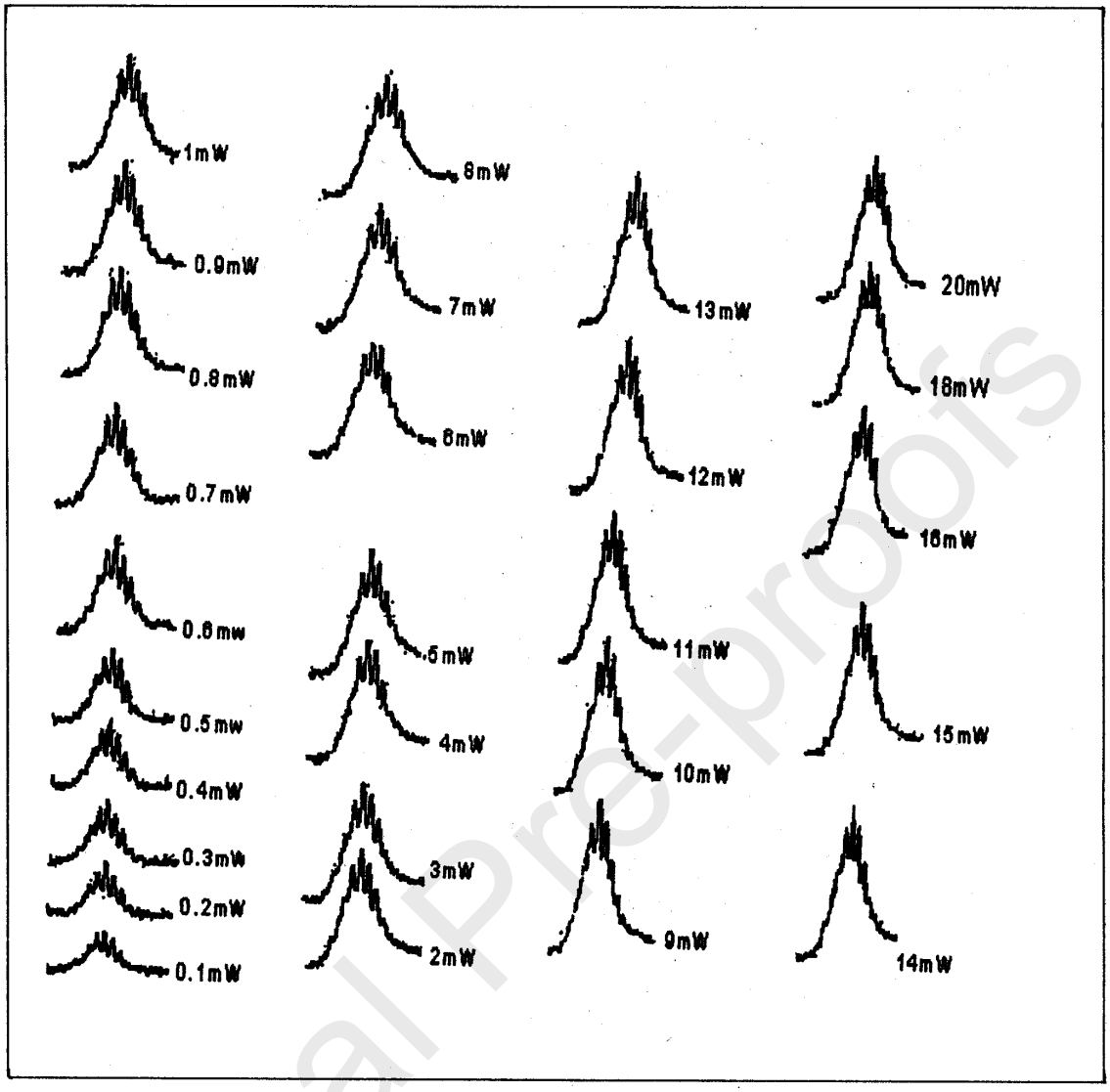

Fig S8e. Representative picture of the EPR Power Saturation spectra of **IX** (0.5 mM) in an ethanolic solution at 77 K at the X-band frequency of 9.0518 GHz in the range 266.0 to 278.0 mT. * represents the peak at 272 mT used for the saturation plot.

An investigation on geometry and metal interactions in multi metallic porphyrin complexes – EPR Studies[microwave power saturation and degree of covalency]

S. Tamijselvy*
School of Basic Sciences, Department of Chemistry, VISTAS, Chennai, TamilNadu-600 117, India.
Corresponding Author Tel: +91 6379647596 Email: tamijselvy@gmail.com

Graphical Abstract

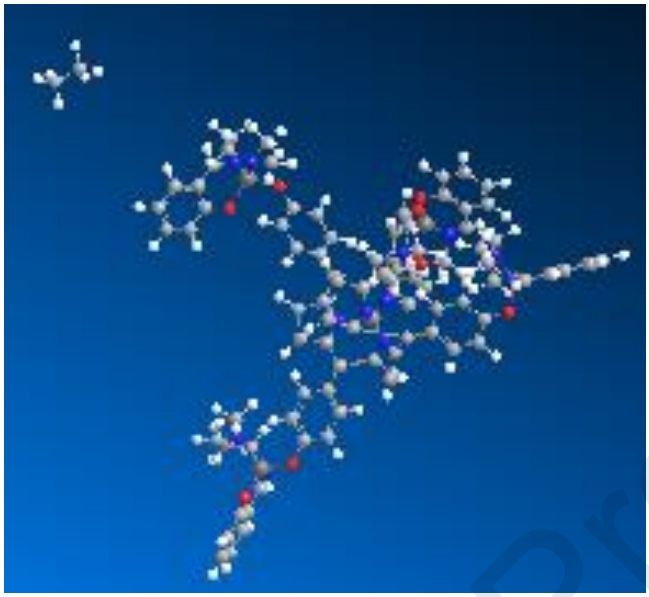

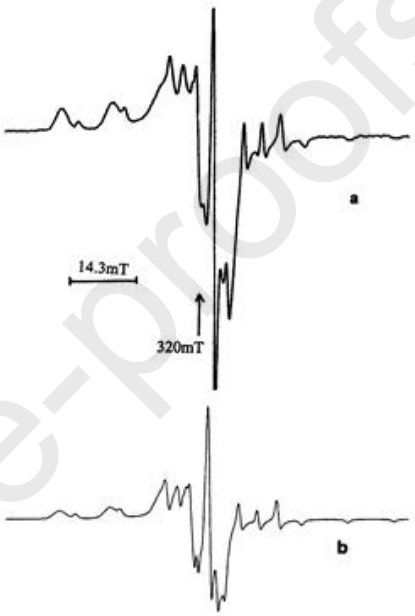

An investigation on geometry and metal interactions in multi metallic porphyrin complexes – EPR Studies [microwave power saturation and degree of covalency]
S. Tamijselvy*
School of Basic Sciences, Department of Chemistry, VISTAS, Chennai, TamilNadu-600 117, India.
Corresponding Author Tel: +91 6379647596 Email: tamijselvy@gmail.com

Graphical Abstract

A series of peripherally copper coordinated metallo-porphyrins were synthesised and their EPR studies reveal clearly the steric hindrance and electronic effects of the substituted groups. The different characteristic nature of the coordinated metal ions plays a major role in inducing the properties of the synthesised complexes and their application in various fields.

An investigation on geometry and metal interactions in multi metallic porphyrin complex – EPR Studies[Microwave power saturation and Degree of covalency]

S. Tamijselvy*

School of Basic Sciences, Department of Chemistry, VISTAS, Chennai, TamilNadu-600 117, India.

Corresponding Author Tel: +91 6379647596 Email: tamijselvy@gmail.com

Author Contributions Section

The article given is the work done by me. Acknowledgement to the persons who helped are included in the manuscript.